

Temporal Evolution of Cognitive Knowledge Networks in AI-Assisted Conversations

Alexander Towell^{1*}, John Matta¹

¹ Department of Computer Science, Southern Illinois University Edwardsville, E

* Corresponding author: atowell@siue.edu

Abstract

How does a person’s knowledge landscape evolve through sustained AI-assisted conversation? We previously introduced a *cognitive MRI* methodology that transforms linear conversation logs into semantic similarity networks, revealing knowledge communities and bridge conversations in a static snapshot [Towell and Matta, 2025]. Here we extend this analysis to the temporal domain, tracking how the network grows over 29 months (December 2022 – April 2025) across 1,908 ChatGPT conversations. We construct cumulative monthly snapshots and discover several evolution patterns characteristic of real-world complex networks. The network exhibits *super-linear densification* ($\gamma = 1.405$, $R^2 = 0.993$), meaning knowledge exploration accelerates as the network grows. New conversations attach to existing topics via *sub-linear preferential attachment* ($\beta = 0.763$, $R^2 = 0.914$), indicating that popular topics attract disproportionate attention but less aggressively than in scale-free models. Community structure stabilizes early (modularity ≈ 0.75 by mid-2023) and persists through subsequent growth, with 40 distinct communities tracked through birth, continuation, and death events. Bridge conversations — critical cross-domain connectors — emerge at identifiable moments and maintain their structural role once established. Comparison across model eras (GPT-3.5 through GPT-

26 4.5) reveals that AI model capabilities shape sub-network topol-
27 ogy. These findings suggest that individual AI-assisted knowledge
28 exploration self-organizes according to the same macroscopic laws
29 observed in collective knowledge systems such as citation and col-
30 laboration networks — but arising through a different mechanism:
31 the progressive revelation of latent semantic structure rather than
32 active social tie formation. This scale-bridging parallel offers both
33 theoretical insight into distributed cognition and practical implica-
34 tions for knowledge management systems.

35 **Keywords:** temporal networks, knowledge networks, AI con-
36 versation analysis, network evolution, densification law, preferential
37 attachment, community dynamics

38 1 Introduction

39 The rise of conversational AI has created a new medium for knowledge
40 exploration. Millions of users now interact daily with large language mod-
41 els (LLMs), generating conversation archives that constitute externalized
42 records of cognitive activity [Zhao et al., 2023]. These archives are typi-
43 cally presented as flat, chronological lists — a format that conceals the rich
44 associative structure latent in accumulated inquiry.

45 In prior work, we introduced a *cognitive MRI* methodology that trans-
46 forms such archives into semantic similarity networks, where conversations
47 become nodes and edges connect semantically related pairs [Towell and
48 Matta, 2025]. Analyzing the giant component of a single user’s conver-
49 sation archive (449 of 601 connected conversations at similarity threshold
50 $\theta = 0.9$), we identified 15 knowledge communities, heterogeneous network
51 topology (hub-and-spoke vs. tree-like structures), and three distinct bridge
52 conversation types that facilitate cross-domain knowledge transfer. That
53 analysis, however, treated the network as a static snapshot — collapsing
54 29 months of knowledge exploration into a single graph.

55 This limitation is significant. The *temporal dimension* of knowledge explo-
56 ration is precisely what distinguishes organic human inquiry from static
57 knowledge bases. Questions build on previous questions; interests drift,
58 deepen, and occasionally collide; new AI model capabilities reshape what
59 is possible to explore. A static analysis cannot capture these dynamics.

60 In this paper, we extend the cognitive MRI to the temporal domain, ana-
61 lyzing how the semantic similarity network evolves over 29 monthly snap-
62 shots spanning December 2022 through April 2025. This temporal exten-
63 sion constitutes the core novel contribution beyond the conference paper,
64 addressing three new research questions:

- 65 1. **Growth dynamics:** Does the network densify over time, and if so,
66 does it follow established densification laws?
- 67 2. **Attachment patterns:** How do new conversations attach to the
68 existing network — randomly, preferentially, or through some inter-
69 mediate mechanism?
- 70 3. **Structural persistence:** Do knowledge communities emerge early
71 and persist, or does the community structure remain in flux?

72 Our analysis reveals that this single-user knowledge network exhibits evolu-
73 tion patterns remarkably consistent with those observed in much larger so-
74 cial, biological, and technological networks [Leskovec et al., 2007, Barabási
75 and Albert, 1999, Palla et al., 2007]. Specifically, we find:

- 76 • **Super-linear densification** ($\gamma = 1.405$, $R^2 = 0.993$): edges grow
77 faster than nodes, meaning the network becomes proportionally denser
78 over time.
- 79 • **Sub-linear preferential attachment** ($\beta = 0.763$, $R^2 = 0.914$):
80 high-degree nodes attract new connections disproportionately, but
81 less aggressively than in the Barabási-Albert model.

- 82 • **Early community stabilization:** modularity reaches ~ 0.75 by
83 mid-2023 and remains stable through 18 subsequent months of growth,
84 despite the network tripling in size.
- 85 • **Bridge persistence:** once a conversation achieves bridge status
86 (top-5% betweenness centrality), it maintains that role throughout
87 the observation period.
- 88 • **Model era effects:** sub-networks from different LLM eras exhibit
89 distinct topological signatures.

90 These findings contribute to temporal network theory by providing a new
91 empirical case study — the evolution of a personal knowledge exploration
92 network — and to the emerging field of human-AI interaction by demon-
93 strating that conversational AI usage leaves structured, analyzable traces
94 of cognitive activity. Our framing draws on the distributed cognition tra-
95 dition [Hutchins, 1995, Clark and Chalmers, 1998], viewing the human-AI
96 conversation archive as an externalized cognitive system whose structure
97 reveals patterns of knowledge organization and exploration.

98 The remainder of this paper is organized as follows. Section 2 reviews re-
99 lated work on temporal networks, densification, and community dynamics.
100 Section 3 describes the temporal analysis methodology. Section 4 presents
101 our findings. Section 5 discusses implications and limitations. Section 6
102 concludes.

103 2 Related Work

104 2.1 Temporal Network Evolution

105 The study of how networks evolve over time has revealed universal patterns
106 across diverse domains. Holme and Saramäki [2012] provide a comprehen-
107 sive review of temporal network analysis, distinguishing between *contact*

108 *sequences* (discrete events) and *interval graphs* (persistent connections).
109 Our cumulative snapshot approach falls into the latter category: once a
110 conversation enters the network, it persists permanently, making the net-
111 work monotonically non-decreasing. This models the reality that knowl-
112 edge, once explored, remains part of one’s cognitive landscape.

113 Dorogovtsev and Mendes [2002] survey evolution models for growing net-
114 works, identifying preferential attachment, fitness-based growth, and aging
115 as key mechanisms. Albert and Barabási [2002] provide a broader statis-
116 tical mechanics perspective on complex network evolution, including the
117 emergence of scale-free properties and small-world characteristics during
118 growth.

119 2.2 Densification Laws

120 Leskovec et al. [2005] discovered that many real-world networks exhibit
121 *densification*: the number of edges grows super-linearly with the number
122 of nodes, following a power law $e(t) \propto n(t)^\gamma$ with $\gamma > 1$. They doc-
123 umented this pattern across citation networks ($\gamma = 1.69$), patent net-
124 works ($\gamma = 1.26$), and autonomous systems graphs ($\gamma = 1.18$), among
125 others [Leskovec et al., 2007]. This contrasts with constant-density growth
126 (Erdős-Rényi) or constant-degree growth (Barabási-Albert, where $\gamma = 1$).
127 Densification implies that as a network grows, participants increasingly
128 find connections to existing content rather than remaining isolated. The
129 exponent γ characterizes how aggressively this acceleration occurs.

130 2.3 Preferential Attachment

131 Barabási and Albert [1999] proposed preferential attachment as a mecha-
132 nism for generating scale-free networks: new nodes connect preferentially
133 to high-degree existing nodes with probability $\Pi(k) \propto k^\beta$. When $\beta = 1$,
134 this produces power-law degree distributions. Jeong et al. [2003] devel-

135 oped methods to measure preferential attachment empirically, finding lin-
136 ear ($\beta \approx 1$) attachment in citation and collaboration networks. Subsequent
137 work has shown that many real networks exhibit *sub-linear* attachment
138 ($\beta < 1$), where high-degree nodes attract connections but not as strongly as
139 the pure model predicts [Newman, 2001]. Sub-linear attachment produces
140 networks with more moderate degree heterogeneity than pure scale-free
141 networks.

142 **2.4 Community Dynamics**

143 Palla et al. [2007] pioneered the study of community evolution in tem-
144 poral networks, tracking overlapping communities in mobile phone and
145 collaboration networks. They identified key lifecycle events: birth, growth,
146 contraction, merging, splitting, and death. Greene et al. [2010] proposed
147 event-based frameworks for tracking non-overlapping communities across
148 snapshots using set overlap measures. Mucha et al. [2010] introduced mul-
149 tiscale community detection for time-dependent networks using generalized
150 modularity optimization. Rossetti and Cazabet [2018] survey the broader
151 field of dynamic community discovery, cataloging approaches from incre-
152 mental methods to tensor decompositions.

153 A key finding across this literature is that community structure in growing
154 networks tends to *stabilize*: after an initial transient period, the mesoscale
155 organization persists even as the microscale (individual nodes and edges)
156 continues to change [Palla et al., 2007].

157 **2.5 Knowledge and Citation Network Evolution**

158 Citation networks provide a natural comparison for knowledge exploration
159 networks. de Solla Price [1965] first studied their growth dynamics, and
160 subsequent work has characterized their densification [Leskovec et al., 2007],
161 preferential attachment [Jeong et al., 2003], and community structure [Chen

162 et al., 2010]. Shi et al. [2015] model the evolution of scientific knowl-
163 edge as a dynamic network, finding that the structure of science exhibits
164 path-dependent growth with both conservative (within-field) and innova-
165 tive (cross-field) exploration patterns. Our work extends this paradigm
166 from collective scientific knowledge to individual knowledge exploration
167 through AI conversation.

168 **2.6 AI Conversation Analysis**

169 Research on AI conversational data has primarily focused on dialogue qual-
170 ity, user satisfaction, and topic modeling [Serban et al., 2016]. Network-
171 based approaches to conversation analysis remain rare. Our conference
172 paper [Towell and Matta, 2025] introduced the first complex network anal-
173 ysis of a personal AI conversation archive, treating conversations as nodes
174 in a semantic similarity network. The present work extends this to the
175 temporal domain, a direction identified as key future work in the original
176 paper.

177 **3 Methods**

178 We describe the temporal analysis methodology that extends our static
179 conference paper analysis [Towell and Matta, 2025]. The base network
180 construction (embedding generation, similarity computation, threshold se-
181 lection) is unchanged; we refer readers to the conference paper for those
182 details and summarize the essentials here.

183 **3.1 Dataset and Base Network**

184 The dataset comprises 1,908 ChatGPT conversations generated by one of
185 the authors between December 2022 and April 2025. Conversations were
186 conducted for authentic research, learning, and problem-solving purposes

187 with no anticipation of future network analysis. Each conversation was em-
 188 bedded using `nomic-embed-text` [Nussbaum et al., 2024] with a 2:1 user:AI
 189 message weighting ratio ($\alpha = 2$), validated through a 63-configuration ab-
 190 lation study [Towell and Matta, 2025]. Pairwise cosine similarities were
 191 computed and filtered at threshold $\theta = 0.9$, yielding 601 connected nodes
 192 and 1,718 edges across 59 connected components, with a giant component
 193 of 453 nodes (1,307 conversations remain isolated at this threshold). The
 194 conference paper [Towell and Matta, 2025] analyzed the giant component
 195 (449 nodes at the time of that analysis); the present work analyzes all
 196 connected nodes.

197 Each conversation carries a creation timestamp, enabling temporal order-
 198 ing. Conversations span five model eras based on the underlying LLM:
 199 GPT-3.5 (pre-GPT-4, $n = 1,214$), GPT-4 ($n = 44$), GPT-4o ($n = 453$),
 200 Reasoning models (o1/o3 series, $n = 181$), and GPT-4.5 ($n = 16$).

201 3.2 Cumulative Temporal Snapshots

202 We construct the network’s temporal evolution through cumulative monthly
 203 snapshots. For each month t in the observation period, the snapshot
 204 $G(t) = (V(t), E(t))$ contains:

$$V(t) = \{v \in V \mid \text{created}(v) \leq \text{end}(t)\} \quad (1)$$

$$E(t) = \{(u, v) \in E \mid u \in V(t) \wedge v \in V(t)\} \quad (2)$$

205 This cumulative construction models the irreversibility of knowledge ex-
 206 ploration: conversations, once created, permanently enrich the knowledge
 207 landscape. It produces 29 monthly snapshots (December 2022 through
 208 April 2025), growing from 1 node to the full 1,908.

209 For each snapshot, we compute a comprehensive set of network metrics
 210 on the connected subgraph: node count, edge count, density, number of

211 connected components, giant component size and fraction, mean and max-
 212 imum degree, average clustering coefficient, transitivity, average shortest
 213 path length (within the giant component), Louvain modularity and com-
 214 munity count [Blondel et al., 2008], average betweenness centrality, and
 215 degree assortativity. Community detection uses a fixed random seed for
 216 reproducibility.

217 For visualization and narrative purposes, we divide the 29-month observa-
 218 tion period into five temporal phases based on usage intensity and model
 219 availability: *Early* (December 2022 – February 2023; 59 conversations, net-
 220 work bootstrapping), *Exploration* (March – July 2023; 635 conversations,
 221 rapid growth), *Established* (August 2023 – January 2024; 402 conversa-
 222 tions, structural consolidation), *GPT-4o* (February – September 2024; 396
 223 conversations, new model capabilities), and *Reasoning* (October 2024 –
 224 April 2025; 416 conversations, reasoning model era). These phases appear
 225 as background shading in several figures.

226 3.3 Community Lifecycle Tracking

227 To track community identity across snapshots, we apply Louvain commu-
 228 nity detection independently at each time step and align communities be-
 229 tween consecutive snapshots using Jaccard similarity of node sets [Jaccard,
 230 1912, Greene et al., 2010].

231 The tracking algorithm (Algorithm 1) proceeds in five passes per transition.
 232 First, for each pair of consecutive communities (C_{t-1}^i, C_t^j) , we compute the
 233 Jaccard index $J(C_{t-1}^i, C_t^j) = |C_{t-1}^i \cap C_t^j| / |C_{t-1}^i \cup C_t^j|$. Communities are
 234 then classified:

- 235 • **Continuation:** C_t^j has a unique best match C_{t-1}^i with $J \geq 0.3$, and
 236 vice versa. The tracked identity is preserved.
- 237 • **Birth:** C_t^j has no match ≥ 0.3 with any previous community. A new
 238 tracked identity is assigned.

Algorithm 1 Community Lifecycle Tracking via Jaccard Alignment

Require: Community partitions $\{P_1, P_2, \dots, P_T\}$, threshold $\tau = 0.3$

Ensure: Tracked communities with lifecycle events

```
1:  $next\_id \leftarrow 0$ 
2: for  $t \leftarrow 2$  to  $T$  do
3:   Compute Jaccard matrix  $J[i, j] = |C_{t-1}^i \cap C_t^j| / |C_{t-1}^i \cup C_t^j|$ 
4:   Pass 1 (Continuations): Match pairs where  $\arg \max_j J[i, j] = j^*$ 
   and  $\arg \max_i J[i, j^*] = i$  and  $J[i, j^*] \geq \tau$ 
5:   Pass 2 (Merges): Detect  $N:1$  mappings among unmatched communities
6:   Pass 3 (Splits): Detect  $1:N$  mappings among unmatched communities
7:   Pass 4 (Births): Assign new  $tracked\_id$  to unmatched current communities
8:   Pass 5 (Deaths): Record unmatched previous communities as dissolved
9: end for
```

239 • **Death:** C_{t-1}^i has no match ≥ 0.3 with any current community. The
240 tracked identity is recorded as dissolved.

241 • **Merge:** Multiple previous communities' best match is the same cur-
242 rent community.

243 • **Split:** One previous community maps to multiple current communi-
244 ties.

245 Each tracked community is labeled with a dominant topic based on key-
246 word analysis of constituent conversation titles (e.g., ML/AI, Program-
247 ming, Statistics, Philosophy, Health, Networks).

248 3.4 Preferential Attachment Analysis

249 To test whether new conversations preferentially attach to high-degree ex-
250 isting nodes, we analyze each monthly transition. For month t , we identify
251 new nodes $V_{\text{new}}(t) = V(t) \setminus V(t-1)$ and new edges incident to these nodes
252 in the existing network $G(t-1)$. For each existing node $v \in V(t-1)$, we
253 compute the fraction of new nodes that connect to it and correlate this
254 with v 's degree in $G(t-1)$.

255 To assess statistical significance, we compare the observed degree–attachment
256 correlation against a null model of uniform random attachment using 1,000
257 permutation tests per month. We compute a z -score indicating how many
258 standard deviations the observed correlation exceeds the null expectation.

259 To quantify the attachment kernel, we pool data across all months and
260 bin existing nodes by degree. For each bin, we compute the empirical
261 attachment probability $\Pi(k)$ (fraction of nodes at degree k that receive at
262 least one new connection). We then fit the power-law kernel:

$$\Pi(k) \propto k^\beta \tag{3}$$

263 where $\beta = 0$ corresponds to uniform random attachment, $\beta = 1$ to linear
264 preferential attachment (Barabási-Albert model), and intermediate values
265 indicate sub-linear preferential attachment.

266 3.5 Densification Law Analysis

267 Following Leskovec et al. [2005], we test whether the network exhibits den-
268 sification by fitting a power law in the log-log space of connected nodes
269 versus edges:

$$e(t) \propto n(t)^\gamma \tag{4}$$

270 where $n(t) = |V_{\text{connected}}(t)|$ and $e(t) = |E(t)|$ are the number of connected
271 nodes and edges at time t . The exponent $\gamma > 1$ indicates super-linear
272 densification (the network becomes proportionally denser), $\gamma = 1$ indicates
273 constant average degree, and $\gamma < 1$ indicates sparsification.

274 We fit this relationship using ordinary least squares (OLS) regression on the
275 log-transformed data, reporting the exponent γ , coefficient of determina-
276 tion R^2 , and p -value. We note that OLS on log-transformed data is an ap-
277 proximation; more rigorous power-law fitting methods exist [Clauset et al.,
278 2009], but OLS is standard practice for densification analysis [Leskovec
279 et al., 2007] and sufficient given our high R^2 values. We exclude early

280 months with fewer than 4 connected nodes where metrics are unstable.

281 An important methodological consideration: because our edges derive from
282 a pre-computed similarity matrix, the densification we observe reflects the
283 *progressive revelation* of latent semantic structure rather than the *creation*
284 of new connections (as in social networks where people actively form ties).
285 We discuss the implications of this distinction in Section 5.3.

286 **3.6 Bridge Formation Dynamics**

287 The conference paper identified five bridge conversations with high be-
288 tweenness centrality that facilitate cross-domain knowledge transfer [Towell
289 and Matta, 2025]. We track these bridges over time, computing normalized
290 betweenness centrality and the number of distinct neighbor communities at
291 each snapshot from each bridge’s creation month onward. A bridge is con-
292 sidered to have achieved “bridge status” when its betweenness centrality
293 enters the top 5% of all nodes.

294 **3.7 Model Era Sub-Network Comparison**

295 To assess whether AI model capabilities influence network topology, we
296 construct separate sub-networks for each model era. Each sub-network
297 contains only conversations from that era and only edges between them. We
298 compute standard network metrics for each era’s sub-network and compare
299 structural signatures across eras.

Network Growth Over 29 Months

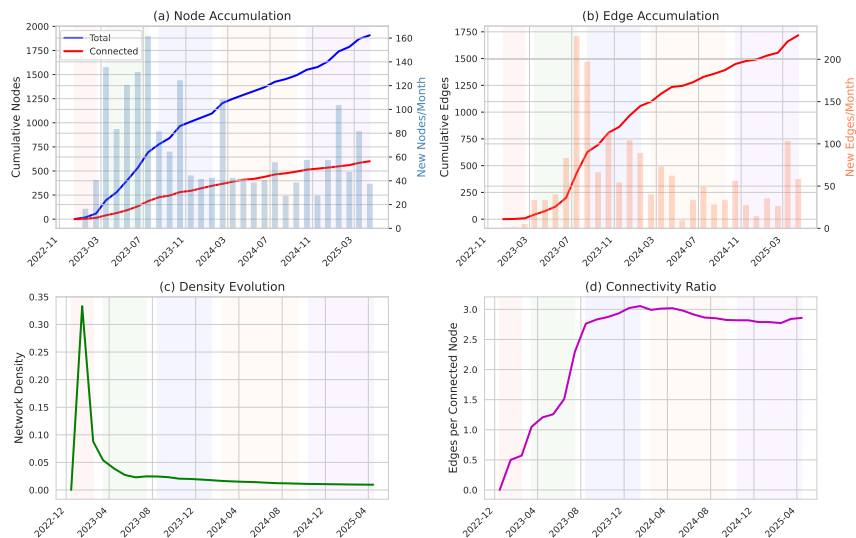


Figure 1: **Network growth over 29 months.** (a) Cumulative node count with monthly additions (bars). (b) Cumulative edge count with monthly additions. (c) Network density over time. (d) Edges per connected node, showing the network becoming proportionally denser despite decreasing density. Background shading indicates five temporal phases: Early (Dec 2022 – Feb 2023), Exploration (Mar – Jul 2023), Established (Aug 2023 – Jan 2024), GPT-4o (Feb – Sep 2024), and Reasoning (Oct 2024 – Apr 2025).

300 4 Results

301 4.1 Network Growth Patterns

302 Figure 1 shows the network’s growth over 29 months. Total conversations
 303 grow from 1 (December 2022) to 1,908 (April 2025), with a rapid expansion
 304 phase from March through July 2023 (averaging 135 new conversations per
 305 month) followed by steadier growth (averaging 54 per month thereafter).
 306 Of the 1,908 total conversations, 601 (31.5%) appear in the connected
 307 network at $\theta = 0.9$.

308 Edge growth outpaces node growth throughout the observation period.
 309 The edges-per-node ratio increases from 0.5 (January 2023) to 2.86 (April
 310 2025), confirming that the network becomes proportionally denser over
 311 time. This trend persists even as absolute density decreases (from 0.33 to

Structural Evolution of the Knowledge Network

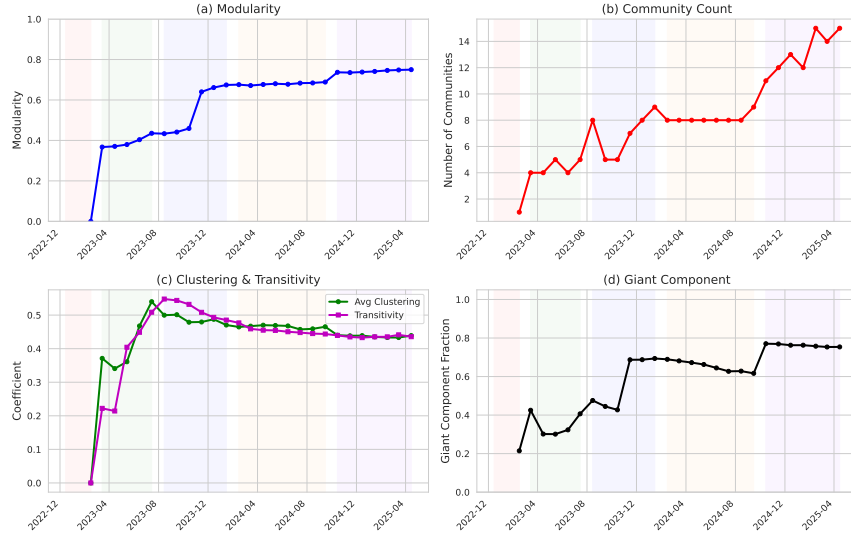


Figure 2: **Structural evolution of network properties.** (a) Modularity stabilizes at ~ 0.75 by late 2023. (b) Community count grows gradually from 1 to 15. (c) Clustering coefficient and transitivity remain stable after initial growth. (d) Giant component fraction shows a step increase in November 2023.

312 0.010), because edge count grows faster than the $n(n - 1)/2$ denominator.

313 4.2 Structural Evolution

314 Figure 2 tracks four structural properties over time. Modularity rises
 315 rapidly from 0.0 to 0.44 during the Exploration phase (March–July 2023),
 316 then undergoes a step increase to 0.64 in November 2023 when the giant
 317 component undergoes significant restructuring. From that point onward,
 318 modularity stabilizes around 0.74 and reaches 0.750 at the final snapshot
 319 — matching the conference paper’s static analysis exactly.

320 The number of detected communities grows from 1 to 15 over the ob-
 321 servation period, with most community births occurring before mid-2024.
 322 Clustering coefficient stabilizes around 0.44 and transitivity around 0.44 by
 323 mid-2023, indicating that the local connection pattern — friends-of-friends
 324 tend to be friends — establishes early and persists.

Table 1: **Community lifecycle event summary.** Events tracked across 28 monthly transitions.

Event Type	Count
Continuations	189
Births	40
Deaths	23
Merges	0
Splits	0
Unique communities tracked	40
Surviving to final snapshot	15

325 The giant component fraction exhibits interesting non-monotonic behavior.
 326 It grows to ~ 0.47 during the Exploration phase, drops temporarily, then in-
 327 creases sharply to 0.69 in November 2023 when previously isolated clusters
 328 merge. This step change coincides with the modularity jump, suggesting a
 329 phase transition in the network’s mesoscale organization.

330 4.3 Community Lifecycles

331 Community tracking across 29 snapshots reveals 40 unique tracked com-
 332 munities, of which 15 survive to the final snapshot (Table 1). The lifecycle
 333 analysis recorded 189 continuation events, 40 births, and 23 deaths. No
 334 merge or split events were detected at the Jaccard threshold of $J = 0.3$,
 335 suggesting that communities in this network grow and dissolve rather than
 336 recombining.

337 Figure 3 shows the community timeline. Several patterns emerge. First,
 338 the largest communities (ML/AI, Statistics, Philosophy) are among the
 339 earliest born and persist throughout the observation period, consistent with
 340 the “first-mover advantage” observed in other temporal community stud-
 341 ies [Palla et al., 2007]. Second, community births are distributed across
 342 the entire period rather than concentrated at the beginning, indicating on-
 343 going diversification of knowledge exploration. Third, community deaths
 344 are concentrated among small, specialized communities that emerge briefly
 345 and dissolve — often subsumed by their larger neighbors as the network

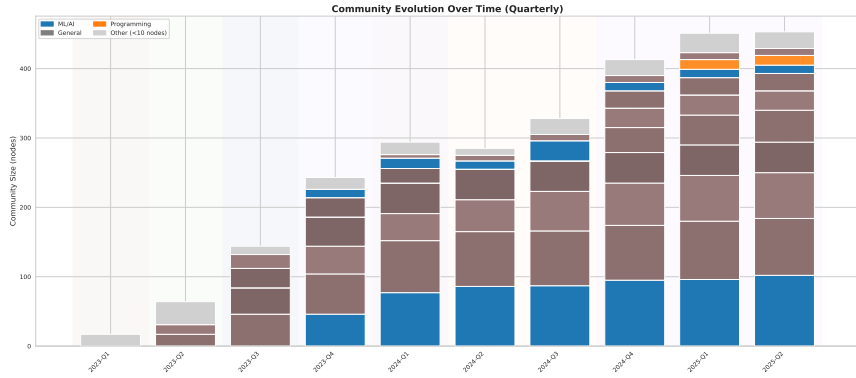


Figure 3: **Community evolution timeline.** Each horizontal band represents a tracked community, colored by dominant topic. Band width indicates community size. Communities are ordered by birth date. The largest communities (ML/AI, General, Statistics) persist throughout the observation period.

346 densifies.

347 The absence of merge and split events is notable. In social networks,
 348 community merging and splitting are common [Palla et al., 2007]. Their
 349 absence here may reflect the nature of knowledge domains: topics like
 350 “machine learning” and “statistics” are cognitively distinct categories that
 351 grow internally rather than fusing, unlike social groups whose membership
 352 boundaries are more fluid.

353 4.4 Densification Law

354 The relationship between connected nodes and edges follows a power law
 355 with remarkable fidelity (Figure 4). Fitting $\log e(t) = \gamma \log n(t) + c$ yields:

$$\gamma = 1.405, \quad R^2 = 0.993, \quad p < 10^{-29} \quad (5)$$

356 This super-linear exponent ($\gamma = 1.405$) places our knowledge network in
 357 the company of other densifying real-world networks, albeit with a mod-
 358 erate exponent. Table 2 compares our result with previously reported
 359 densification exponents.

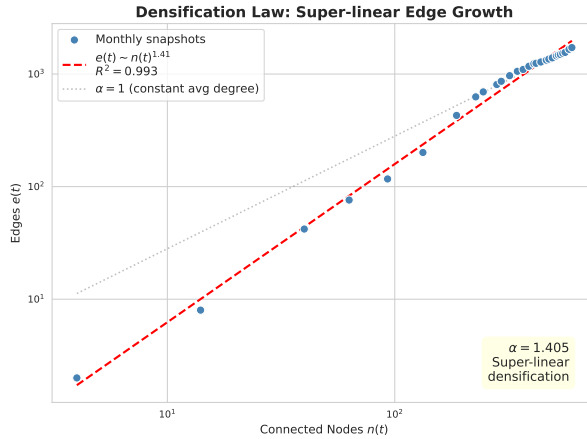


Figure 4: **Densification law.** Log-log plot of edges versus connected nodes across 28 monthly snapshots. The fitted power law $e(t) \propto n(t)^{1.405}$ (dashed line) fits the data with $R^2 = 0.993$, indicating super-linear densification.

Table 2: **Densification exponents across network types.** Our knowledge network exhibits moderate super-linear densification comparable to patent and social networks.

Network	Exponent γ	Source
arXiv citations	1.69	Leskovec et al. [2007]
Patent citations	1.26	Leskovec et al. [2007]
Autonomous systems	1.18	Leskovec et al. [2007]
Knowledge network (this work)	1.405	—

360 The exponent $\gamma = 1.405$ indicates that for every doubling of the connected
361 node count, the edge count increases by a factor of $2^{1.405} \approx 2.65$. This
362 acceleration reflects the increasing semantic interconnectedness of conver-
363 sations as the knowledge landscape fills in: later conversations are more
364 likely to find existing semantic neighbors than early ones, because there
365 are more potential neighbors in a richer knowledge base.

366 4.5 Preferential Attachment

367 Figure 5 presents the preferential attachment analysis. The degree–attachment
368 correlation is consistently positive and significantly exceeds the null model
369 of random attachment across nearly all months. The median z -score is
370 8.5 (range: 0.5–13.2), indicating strong statistical evidence for preferential
371 attachment.

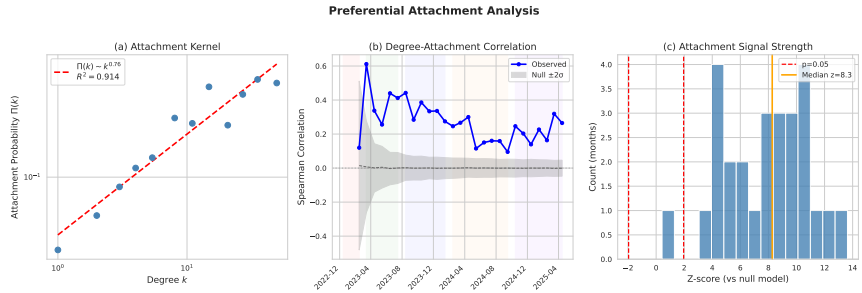


Figure 5: **Preferential attachment analysis.** (a) Attachment kernel $\Pi(k)$ versus degree k on log-log axes, with fitted power law $\Pi(k) \propto k^{0.763}$. (b) Monthly degree–attachment correlation (black) versus null model distribution (gray band shows mean $\pm 2\sigma$). (c) Distribution of z -scores across months, consistently exceeding the significance threshold.

372 The pooled attachment kernel follows a power law $\Pi(k) \propto k^\beta$ with:

$$\beta = 0.763, \quad R^2 = 0.914 \quad (6)$$

373 This sub-linear exponent ($0 < \beta < 1$) indicates that high-degree nodes at-
 374 tract disproportionately many new connections, but less aggressively than
 375 pure preferential attachment ($\beta = 1$). This is consistent with the ob-
 376 servation from the conference paper that our network exhibits “evolution
 377 beyond preferential attachment, reflecting cognitive exploration with hub
 378 formation limited by specialization and cross-domain constraints” [Towell
 379 and Matta, 2025]. The sub-linear kernel produces networks with moderate
 380 degree heterogeneity — broad-tailed degree distributions without extreme
 381 hubs — matching the empirical degree distribution observed in our net-
 382 work.

383 The month-by-month correlation shows temporal variation. The Explo-
 384 ration phase (March–July 2023) exhibits the strongest preferential attach-
 385 ment ($z > 8$), possibly because rapid growth leads new conversations to
 386 cluster around established topics. Later months show reduced but still
 387 significant preferential attachment, consistent with diversification into new
 388 topics.

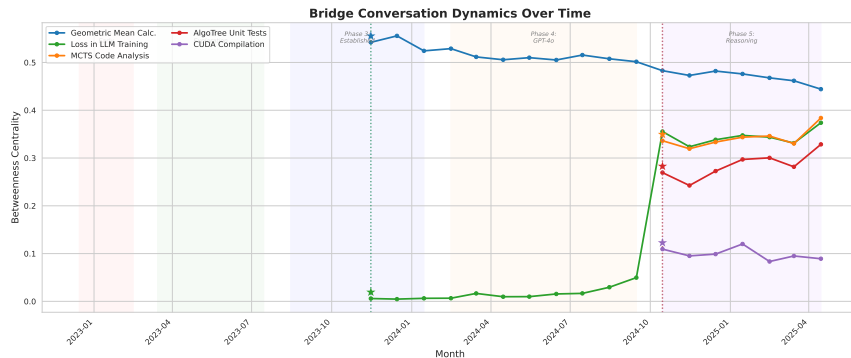


Figure 6: **Bridge formation dynamics.** Normalized betweenness centrality over time for the five bridge conversations identified in the conference paper. Vertical dashed lines mark creation dates. The “geometric-mean-calculation” bridge dominates throughout, while other bridges emerge later and stabilize at lower centrality levels.

389 4.6 Bridge Formation Dynamics

390 Figure 6 tracks the five bridge conversations identified in the conference pa-
 391 per over time. The most striking pattern is the *dominance and persistence*
 392 of the primary bridge, `geometric-mean-calculation`, which achieves bridge
 393 status immediately upon appearing in the connected network (November
 394 2023) and maintains normalized betweenness centrality above 0.44 through-
 395 out the remaining 18 months. This conversation, which evolved from geo-
 396 metric means into probability theory and neural networks, exemplifies the
 397 “evolutionary bridge” type from the conference paper taxonomy.

398 The second bridge, `loss-in-llm-training`, enters the connected net-
 399 work in November 2023—the same month as the primary bridge—but
 400 with low initial betweenness centrality (0.006). It achieves bridge sta-
 401 tus only in September 2024, when its centrality jumps to 0.045 as it
 402 begins connecting multiple communities. The remaining three bridges
 403 (`mcts-code-analysis-suggestions`, `algotree-generate-unit-tests-flattree`,
 404 `compile-cuda-program-linux`) enter in October 2024, coinciding with
 405 the expansion of the giant component during the Reasoning model era.
 406 Once established, each maintains a stable betweenness centrality level:
 407 `mcts-code-analysis-suggestions` and `loss-in-llm-training` stabilize

Table 3: **Sub-network metrics by model era.** Each era’s sub-network contains only conversations from that era and edges between them.

Era	Connected	Edges	Avg. Degree	Clustering	Modularity
GPT-3.5	360	1,102	6.12	0.381	0.675
GPT-4	15	10	1.33	0.156	0.001
GPT-4o	112	148	2.64	0.290	0.670
Reasoning	32	27	1.69	0.168	0.353
GPT-4.5	2	1	—	—	—

408 around 0.35, `algotree-generate-unit-tests-flattree` around 0.30, and
 409 `compile-cuda-program-linux` around 0.09–0.12.

410 The stability of bridge centrality over time — once established, bridges
 411 maintain their structural role — suggests that the cross-domain connec-
 412 tions they provide are not incidental but reflect genuine semantic bridging
 413 between knowledge communities.

414 The bridge conversations span 2–5 neighbor communities each. The `geometric-`
 415 `mean-calculation` bridge consistently connects 4 communities, confirming
 416 its role as a multi-domain integrator. In contrast, `compile-cuda-program-`
 417 `linux` connects exactly 2 communities throughout its tracked lifetime, ex-
 418 emplifying the “pure bridge” type: a minimal but critical link between
 419 domains.

420 4.7 Model Era Effects

421 Table 3 presents sub-network metrics for each model era. The GPT-3.5 era
 422 dominates the dataset (1,214 conversations, 360 connected) and naturally
 423 produces the largest, most structured sub-network (modularity 0.675, 7
 424 communities). The GPT-4o era, despite fewer conversations (453 total,
 425 112 connected), produces a recognizable community structure (modularity
 426 0.668, 6 communities).

427 The Reasoning era (o1/o3 models, 181 conversations, 32 connected) shows
 428 notably lower modularity (0.353) than GPT-3.5 or GPT-4o eras. This

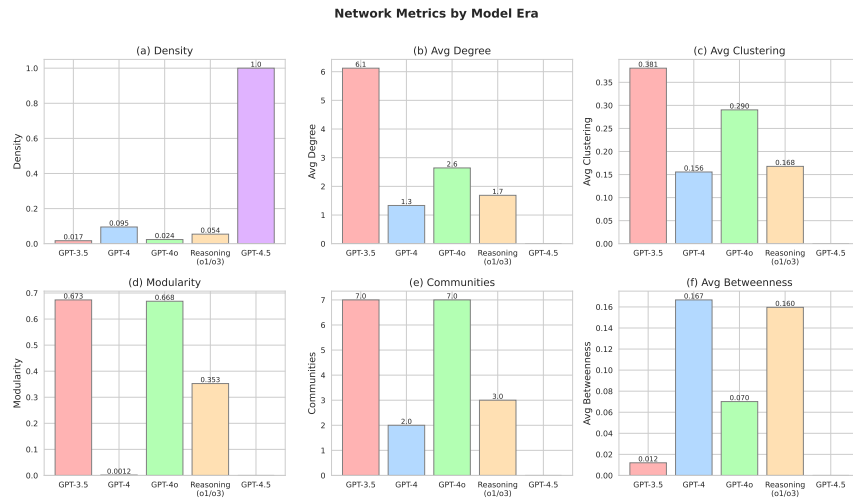


Figure 7: **Model era sub-network comparison.** Network metrics for sub-networks constructed from conversations within each model era. GPT-3.5 and GPT-4o eras produce the richest internal structure.

429 may reflect the nature of reasoning model usage: these models are often
 430 applied to focused, technical problems that span traditional topic bound-
 431 aries, producing more topically diffuse conversations. Alternatively, the
 432 smaller sample size may simply be insufficient for well-defined community
 433 structure to emerge.

434 The GPT-4 and GPT-4.5 eras contain too few connected conversations for
 435 meaningful structural analysis (15 and 2, respectively). The small GPT-4
 436 sample is a metadata artifact: ChatGPT’s export format did not record the
 437 model field until approximately March 2024, so earlier GPT-4 conversations
 438 appear as `None` and are grouped with the GPT-3.5 era. The 44 explicitly
 439 labeled GPT-4 conversations represent only the brief window (March–May
 440 2024) before GPT-4o became the default. The GPT-4.5 era is small due
 441 to low usage by the author.

442 5 Discussion

443 5.1 Cognitive Interpretation

444 The temporal evolution patterns we observe can be interpreted through
445 the lens of distributed cognition [Hutchins, 1995] and the extended mind
446 thesis [Clark and Chalmers, 1998]. The conversation archive functions
447 as an externalized cognitive system, and its growth dynamics reveal how
448 knowledge exploration self-organizes over time.

449 The super-linear densification ($\gamma = 1.405$) has a natural cognitive interpre-
450 tation: as one’s knowledge base grows, new inquiries increasingly connect
451 to existing knowledge rather than standing alone. This reflects the cumula-
452 tive nature of learning — later conversations benefit from a richer contex-
453 tual landscape, making semantic connections more likely. The densification
454 exponent quantifies the *rate* at which knowledge becomes interconnected.

455 Sub-linear preferential attachment ($\beta = 0.763$) suggests a balanced explo-
456 ration strategy. Popular topics (high-degree nodes) do attract follow-up
457 conversations, but the sub-linear kernel indicates that the user also explores
458 less-established topics rather than exclusively deepening existing interests.
459 This balances *exploitation* (deepening known topics) with *exploration* (in-
460 vestigating new ones) — a pattern recognized in the learning sciences and
461 cognitive exploration literature.

462 The early stabilization of community structure (modularity ~ 0.75 by mid-
463 2023, persisting through 18 months) suggests that a user’s knowledge do-
464 mains crystallize relatively quickly. Once the major thematic communities
465 are established, subsequent growth fills in rather than restructures. This is
466 consistent with schema theory in cognitive psychology: once mental frame-
467 works are established, new information is assimilated into existing schemas
468 rather than triggering wholesale reorganization.

469 5.2 Comparison with Known Network Evolution Pat- 470 terns

471 Our findings place this personal knowledge network squarely within the
472 family of densifying, preferentially attaching real-world networks docu-
473 mented by Leskovec et al. [2007] and Barabási and Albert [1999]. The
474 densification exponent ($\gamma = 1.405$) falls between those of patent citation
475 networks ($\gamma = 1.26$) and arXiv citation networks ($\gamma = 1.69$), suggesting
476 comparable but not identical growth dynamics. The sub-linear preferential
477 attachment ($\beta = 0.763$) is lower than the near-linear values reported for
478 citation networks [Jeong et al., 2003], consistent with the conference pa-
479 per’s observation that hub formation is limited by cognitive specialization
480 constraints.

481 The community lifecycle patterns — persistent major communities, gradual
482 births, no merges or splits — differ from social networks where community
483 fusion and fission are common [Palla et al., 2007]. This distinction likely re-
484 flects the fundamental difference between social identity (fluid, negotiated)
485 and knowledge domain identity (more stable, ontologically grounded). A
486 “machine learning” community and a “statistics” community may grow
487 closer as related conversations accumulate, but they do not merge in the
488 way social groups do.

489 The temporal analysis also provides a developmental account of the het-
490 erogeneous topology described in the conference paper [Towell and Matta,
491 2025], where theoretical domains (ML/AI, Statistics, Philosophy) exhib-
492 ited dense hub-and-spoke structures while practical domains (Program-
493 ming) showed sparser, tree-like hierarchies. Community tracking reveals
494 that this heterogeneity has a temporal origin: the theoretical communities
495 are among the earliest born and have the longest growth histories, ac-
496 cumulating dense internal connections through sustained exploration over
497 20+ months. In contrast, practical communities tend to emerge later and
498 grow through independent, focused conversations that branch rather than

499 cluster. The sub-linear preferential attachment we measure ($\beta = 0.763$)
500 quantifies the mechanism the conference paper observed qualitatively —
501 hubs form, but their growth is limited by cognitive specialization, pro-
502 ducing the moderate degree heterogeneity rather than extreme scale-free
503 structure.

504 5.3 The Densification Paradox

505 An important caveat applies to the densification finding. In social net-
506 works, densification reflects the active formation of new ties. In our net-
507 work, edges derive from a pre-computed similarity matrix: all potential
508 connections exist latently from the moment both endpoints are created.
509 The “densification” we observe is actually the *progressive revelation* of la-
510 tent structure as the network fills in.

511 This distinction matters for interpretation but does not invalidate the find-
512 ing. The densification law still accurately describes the growth trajectory
513 and has predictive value: it tells us that later additions to the conversa-
514 tion archive will be proportionally more connected than earlier ones. The
515 mechanism, however, is not active tie formation but rather the increas-
516 ing density of the semantic space being sampled. As more conversations
517 are added to more topics, new conversations are more likely to land near
518 existing ones in semantic space.

519 We note that a similar argument applies to any threshold-based similarity
520 network, including many co-occurrence and co-citation networks. The den-
521 sification patterns reported by Leskovec et al. [2007] for citation networks
522 also involve retrospectively computed relationships rather than active so-
523 cial ties. Our case makes this mechanism particularly transparent.

524 5.4 Implications

525 Our findings have practical implications for the design of knowledge man-
526 agement and conversation archival systems:

- 527 1. **Community-aware organization:** The early stabilization of com-
528 munity structure suggests that knowledge domains can be identified
529 relatively early in a user’s conversation history and used to organize
530 archives thematically.
- 531 2. **Bridge surfacing:** The persistence of bridge conversations once es-
532 tablished suggests that identifying bridges early could help users dis-
533 cover cross-domain connections.
- 534 3. **Densification-aware retrieval:** The densification law implies that
535 retrieval systems should expect increasing connectivity over time, po-
536 tentially enabling richer recommendation strategies as the archive
537 grows.
- 538 4. **Model-aware analysis:** The distinct topological signatures across
539 model eras suggest that AI model capabilities influence knowledge
540 structure, which may be relevant for understanding how AI tools
541 shape thinking patterns.

542 5.5 Limitations

543 Several limitations constrain the generalizability of our findings.

544 **Single user.** This remains a case study of one user’s conversation archive.
545 While we demonstrate that the methodology produces meaningful and con-
546 sistent results, the specific parameter values (γ , β , community count, etc.)
547 may differ for other users. Multi-user studies are needed to establish which
548 patterns generalize.

549 **Pre-computed similarities.** As discussed in Section 5.3, edges are de-

550 terminated by semantic similarity rather than active social choice. The den-
551 sification we observe is structurally real but mechanistically different from
552 that in social or collaboration networks.

553 **Embedding model consistency.** The same embedding model (`nomic-embed-text`)
554 was used for all conversations regardless of their creation date. In practice,
555 embedding models may evolve, and conversations from different periods
556 might be better represented by different models.

557 **Louvain non-determinism.** Although we use a fixed random seed,
558 Louvain community detection is inherently non-deterministic across dif-
559 ferent implementations and platforms. Community event counts may vary
560 slightly across runs.

561 **Single threshold.** We analyze the network at a single similarity threshold
562 ($\theta = 0.9$), validated by the conference paper’s ablation study. The temporal
563 patterns at other thresholds remain unexplored.

564 **Model era confounds.** Differences between model era sub-networks may
565 reflect temporal trends (topic interests change over time), model capabili-
566 ties, or both. Furthermore, model era classification relies on export meta-
567 data that was absent before March 2024; the “GPT-3.5” era likely contains
568 an unknown number of GPT-4 conversations. The small labeled GPT-4
569 and GPT-4.5 samples preclude meaningful comparison for those eras.

570 **6 Conclusion**

571 We have extended the cognitive MRI methodology from static to temporal
572 network analysis, tracking how a personal knowledge network grows over
573 29 months of AI-assisted conversation. The network exhibits evolution
574 patterns characteristic of real-world complex systems: super-linear densi-
575 fication ($\gamma = 1.405$), sub-linear preferential attachment ($\beta = 0.763$), early
576 community stabilization, and persistent bridge formation.

577 These findings demonstrate that personal knowledge exploration through
578 conversational AI is not random accumulation but self-organizes accord-
579 ing to the same macroscopic laws that govern collective knowledge sys-
580 tems. Densification quantifies how knowledge becomes increasingly inter-
581 connected; preferential attachment reveals the balance between deepening
582 existing interests and exploring new ones; community tracking shows how
583 knowledge domains crystallize early and persist; bridge dynamics illumi-
584 nate how cross-domain connections form and stabilize. That these patterns
585 emerge at the scale of a single individual — mirroring dynamics previously
586 documented only in multi-agent systems like scientific citation networks
587 and online collaboration platforms — suggests that the organizational prin-
588 ciples of knowledge exploration may be scale-invariant, operating whether
589 the exploring agent is a community of scientists or a single person convers-
590 ing with an AI.

591 The mechanism differs: in our network, densification reflects the progres-
592 sive revelation of latent semantic structure rather than active social tie
593 formation. Yet the resulting growth laws are strikingly similar, raising
594 the question of whether individual and collective knowledge exploration
595 are governed by common underlying dynamics. Multi-user studies will be
596 needed to test this hypothesis. Our methodology provides a template for
597 such investigations, and our findings offer a first empirical characteriza-
598 tion of how one person’s knowledge landscape evolves through sustained
599 AI interaction.

600 Code and data for reproducing this analysis are publicly available [Towell,
601 2025].

602 **Data Availability Statement**

603 The conversation embedding dataset and analysis code are available at [ht](https://github.com/queelius/chatgpt-complex-net)
604 [tps://github.com/queelius/chatgpt-complex-net](https://github.com/queelius/chatgpt-complex-net) (DOI: 10.5281/zen-

605 odo.15314235). Raw conversation content is not shared to protect the pri-
606 vacy of the human participant, but all derived data (embeddings, edges,
607 temporal metrics) needed to reproduce the analyses are included.

608 **Author Contributions**

609 **Alexander Towell:** Conceptualization, Methodology, Software, Formal
610 Analysis, Data Curation, Writing – Original Draft, Visualization. **John**
611 **Matta:** Supervision, Writing – Review & Editing.

612 **Funding**

613 This research received no specific funding from any agency in the public,
614 commercial, or not-for-profit sectors.

615 **Competing Interests**

616 The authors declare no competing interests.

617 **Ethics Statement**

618 This study analyzes one author’s own ChatGPT conversation archive. No
619 human subjects were recruited, and no personally identifiable information
620 about third parties is included in the dataset or analysis. The conversation
621 data was generated through the author’s routine use of a commercially
622 available AI service.

623 Acknowledgments

624 The authors thank the organizers of the PLOS Complex Systems special
625 issue on Complex Networks 2025 for the invitation to submit this extended
626 work.

627 References

628 Alexander Towell and John Matta. Cognitive MRI of AI conversations:
629 Analyzing AI interactions through semantic embedding networks. In
630 *Proceedings of the International Conference on Complex Networks and
631 Their Applications (Complex Networks 2025)*, Studies in Computational
632 Intelligence. Springer, 2025.

633 Wayne Xin Zhao, Kun Zhou, Junyi Li, Tianyi Tang, Xiaolei Wang, Yupeng
634 Hou, Yingqian Min, Beichen Zhang, Junjie Zhang, Zican Dong, et al. A
635 survey of large language models. *arXiv preprint arXiv:2303.18223*, 2023.

636 Jure Leskovec, Jon Kleinberg, and Christos Faloutsos. Graph evolution:
637 Densification and shrinking diameters. *ACM Transactions on Knowledge
638 Discovery from Data*, 1(1):2–es, 2007. doi: 10.1145/1217299.1217301.

639 Albert-László Barabási and Réka Albert. Emergence of scaling in random
640 networks. *Science*, 286(5439):509–512, 1999. doi: 10.1126/science.286.
641 5439.509.

642 Gergely Palla, Albert-László Barabási, and Tamás Vicsek. Quantifying
643 social group evolution. *Nature*, 446(7136):664–667, 2007. doi: 10.1038/
644 nature05670.

645 Edwin Hutchins. *Cognition in the Wild*. MIT Press, 1995.

646 Andy Clark and David Chalmers. The extended mind. *Analysis*, 58(1):
647 7–19, 1998.

648 Petter Holme and Jari Saramäki. Temporal networks. *Physics Reports*,
649 519(3):97–125, 2012. doi: 10.1016/j.physrep.2012.03.001.

650 Sergey N. Dorogovtsev and Jose F. F. Mendes. Evolution of networks.
651 *Advances in Physics*, 51(4):1079–1187, 2002. doi: 10.1080/0001873011
652 0112519.

653 Réka Albert and Albert-László Barabási. Statistical mechanics of complex
654 networks. *Reviews of Modern Physics*, 74(1):47–97, 2002. doi: 10.1103/
655 RevModPhys.74.47.

656 Jure Leskovec, Jon Kleinberg, and Christos Faloutsos. Graphs over time:
657 densification laws, shrinking diameters and possible explanations. In
658 *Proceedings of the 11th ACM SIGKDD International Conference on*
659 *Knowledge Discovery and Data Mining*, pages 177–187, 2005. doi:
660 10.1145/1081870.1081893.

661 Hawoong Jeong, Zoltán Nédá, and Albert-László Barabási. Measuring
662 preferential attachment in evolving networks. *Europhysics Letters*, 61
663 (4):567–572, 2003. doi: 10.1209/epl/i2003-00166-9.

664 Mark E. J. Newman. Clustering and preferential attachment in growing
665 networks. *Physical Review E*, 64(2):025102, 2001. doi: 10.1103/PhysRe
666 vE.64.025102.

667 Derek Greene, Donal Doyle, and Pádraig Cunningham. Tracking the evo-
668 lution of communities in dynamic social networks. In *Proceedings of the*
669 *International Conference on Advances in Social Networks Analysis and*
670 *Mining*, pages 176–183, 2010. doi: 10.1109/ASONAM.2010.17.

671 Peter J. Mucha, Thomas Richardson, Kevin Macon, Mason A. Porter, and
672 Jukka-Pekka Onnela. Community structure in time-dependent, multi-
673 plex, and other multiscale networks. *Science*, 328(5980):876–878, 2010.
674 doi: 10.1126/science.1184819.

675 Giulio Rossetti and Rémy Cazabet. Community discovery in dynamic
676 networks: a survey. *ACM Computing Surveys*, 51(2):1–37, 2018. doi:
677 10.1145/3172867.

678 Derek J. de Solla Price. Networks of scientific papers. *Science*, 149(3683):
679 510–515, 1965. doi: 10.1126/science.149.3683.510.

680 Chaomei Chen, Fidelia Ibekwe-SanJuan, and Jianhua Hou. The structure
681 and dynamics of cocitation clusters: A multiple-perspective cocitation
682 analysis. *Journal of the American Society for Information Science and*
683 *Technology*, 61(7):1386–1409, 2010. doi: 10.1002/asi.21309.

684 Feng Shi, Jacob G. Foster, and James A. Evans. Weaving the fabric of
685 science: Dynamic network models of science’s unfolding structure. *Social*
686 *Networks*, 43:73–85, 2015. doi: 10.1016/j.socnet.2015.02.006.

687 Iulian Vlad Serban, Ryan Lowe, Peter Henderson, Laurent Charlin, and
688 Joelle Pineau. A survey of available corpora for building data-driven
689 dialogue systems. *arXiv preprint arXiv:1512.05742*, 2016.

690 Zach Nussbaum, John X. Morris, Brandon Duderstadt, and Andriy Mul-
691 yar. Nomic embed: Training a reproducible long context text embedder.
692 *arXiv preprint arXiv:2402.01613*, 2024.

693 Vincent D. Blondel, Jean-Loup Guillaume, Renaud Lambiotte, and Etienne
694 Lefebvre. Fast unfolding of communities in large networks. *Journal of*
695 *Statistical Mechanics: Theory and Experiment*, 2008(10):P10008, 2008.
696 doi: 10.1088/1742-5468/2008/10/P10008.

697 Paul Jaccard. The distribution of the flora in the alpine zone. *New Phy-*
698 *tologist*, 11(2):37–50, 1912.

699 Aaron Clauset, Cosma Rohilla Shalizi, and Mark E. J. Newman. Power-law
700 distributions in empirical data. *SIAM Review*, 51(4):661–703, 2009. doi:
701 10.1137/070710111.

702 Alexander Towell. chatgpt-complex-net: Complex network analysis of
703 ChatGPT conversations, 2025. URL [https://github.com/queeliu](https://github.com/queeliums/chatgpt-complex-net)
704 [s/chatgpt-complex-net](https://github.com/queeliums/chatgpt-complex-net).